JCAMECH

Vol. 47, No. 1, June 2016, pp 99-107
DOI: 10.22059/jcamech.2016.59259

Parametric investigation of auto-frettage process in thick spherical vessel made of functionally graded materials

Saeed Farahmand [1], Ali Asghar Atai [2,*]

1- Department of Mechanical Engineering, Karaj Branch, Islamic Azad University, Karaj, Iran
2- School of Mechanical Engineering, College of Engineering, University of Tehran, Iran

Received: 9 Apr. 2016 , Accepted: 14 May 2016

Abstract

In this paper, the effect of autofrettage process parameters on the ultimate pressure that functionally graded spherical vessel can tolerate are investigated. FGM properties and autofrettage pressure are considered as important parameters. Assumptions are variation of properties of FGM in radial direction, the residual stress in the absence of Bauschinger effect with the operation of variable material property method for bilinear material and power law fraction distribution for FG vessel calculated. The stress distribution in loading phase is computed using projection method and rule of mixture for FGM and elastic solution for thick spherical vessel. In unloading phase the material behavior is assumed to be isotropic and residual stress computed by using superposition method for loading and unloading phase. For reloading phase the rules of linear mixture employed for estimating the ultimate strength of FGM. By assuming functionally graded material properties and autofrettage process as effective parameters on amount of pressure capacity of autofrettaged vessel, the effects of parameters discussed separately. The results illustrate considerable effect of volume fraction used in FGM (up to 35**%** compared to full metal case) and inhomogeneity exponent (up to 154% compared to homogeneous case) on amount of ultimate pressure which is mentioned in results of parametric analyzing.

Keywords:

Autofrettage, Residual Stress, Spherical Vessel, FGM, Elasto- plastic analysis, Parametric study

1. Introduction

Autofrettage is a process in which the thick vessel is subjected to high pressure, causing considerable plastic deformation at inner surface of vessel. Autofrettage is mostly used to induce compressive residual stress at the bore of thick walled vessel. The compressive residual stress enhances the fatigue life time and load carrying capacity of the vessel[1]. The plasticity of material cause permanent internal deformation after loading phase in autofrettaged vessel which induced compressive residual stress at inner and

* Corresponding Author. Tel.: +98 123 456789; Fax: +98 123 456789
Email Address: aataee@ut.ac.ir.

tensile residual stress at outer part of the vessel. The material plastic behavior is limited; to overcome this limitation ceramic particle in functionally graded material (FGM) can be used. FGMs, while offering the advantages of composites, avoid the negative effects of abrupt changes in the layered composite material. Using FGM while offering better thermal conductivity and avoiding thermal stress cause better stress distribution in vessel and achieving higher residual stress.

Parker *et al.* [2] investigated residual stress of autofrettage and reautofrettage of homogenous spherical vessel without considering any failure criteria. Farrahi *et al.* [3] investigated residual stress of the autofrettaged thick-walled cylindrical vessel using kinematic hardening behavior for homogenous vessel without considering any failure criteria. Farrahi *et al.* [4] used finite element simulations to simulate reautofrettage process of homogenous thick-walled tube to estimate the residual stress distribution. The study of autofrettage process in spherical vessels was in attention in the recent years. Adibi-asl *et al.* [5] investigated analytical approach in autofrettaged homogenous spherical pressure vessels for calculation of residual stress. Maleki *et al.* [6] investigated residual stress of thick-walled homogenous spherical vessel using variable material property (VMP) method.

Haghpanah Jahromi [7] extended the application of the VMP method to materials with varying elasto-plastic properties and demonstrated its applications to calculate residual stress in an autofrettaged FGM cylindrical vessel. In FGM, ceramic volume fraction varies from inner to outer surface of vessel. Ceramic particle create higher elastic modulus in outer surface of FGM vessel that cause less strain distribution for outer surface which Eventuated more compressive residual stress at inner surface and tensile residual stress at outer surface of FG vessel compare to homogenous metal vessel. The study of autofrettage technique in vessel has been the subject of several research works. In previous researches, autofrettage process for FG vessel investigated for linear distribution of ceramic particle in thickness of vessel without considering any failure criteria for estimating pressure capacity in reloading of the autofrettaged vessel that makes research away from applied industry. In this research the effects of using ceramic particle on pressure capacity of vessel are investigated. Although ceramic particle offering higher residual stress but because of its lower tensile ultimate strength compare to metal, it cause drop in vessel pressure capacity. In this research the FGM behavior (consist the amount of ceramic particle) and autofrettage pressure are assumed as effective parameters for finding beneficial mount of ceramic particle in FGM. In loading phase of autofrettage process the Von Mises criteria employed for prediction of vessel failure. Development of VMP method and residual stress formulation for spherical FG vessel are presented in sections 2 and 3 respectively. The FG material model is presented in section 4. Validation of model for a homogeneous case and a thorough paramtere study of the process are presented in section 5.

2. Variable Material Property

This method was introduced by Jahed and Dubey [8] in 1997. It is based on using elastic solution as inelastic solution. Fig. 1 shows, by increasing internal pressure of vessel with inner radius of r_i and outer radius of r_o the inner surface change to plastic form and plastic region is developed through thickness of vessel which induced beneficial compressive residual stress at inner part of vessel. In this method the vessel divided to several thin strip elements and each thin element assumed to be homogenous.

2.1. *Formulation*

For each strip elastic strain and plastic strain shown by ε_{ij}^{e} and ε_{ij}^{p} respectively. According to Hooke's law the elastic strain shows in Eq. (1)

$$\varepsilon_{ij}^{e} = \frac{1+v(x)}{E(x)}\sigma_{ij} - \frac{v(x)}{E(x)}\sigma_{kk}\delta_{ij} \quad (1)$$

In which δ_{ij}, $E(x)$ and $v(x)$ are Kronecker delta, elastic modulus and Poisson ratio for each strip, respectively. Plastic strain according to Hencky's law is proposed with Eq. (2).

$$\varepsilon_{ij}^{p} = \Phi\, s_{ij} \quad (2)$$

In which s_{ij} is deviatoric stress that shows in Eq. (3).

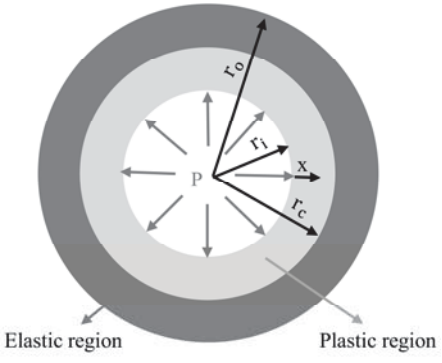

Fig. 1. Schematic of vessel under autofrettage pressure with elastic- plastic region

$$s_{ij} = \sigma_{ij} - \frac{1}{3}\sigma_{kk}\delta_{ij} \quad (3)$$

And Φ is scalar function as given in Eq. (4)

$$\Phi = \frac{3}{2}\frac{\varepsilon_{eq}^{p}}{\sigma_{eq}} \quad (4)$$

ε_{eq}^{p} and σ_{eq} are equivalent plastic strain and equivalent stress. Using Eq. (1), Eq. (2) and Eq. (3) the total strain obtained by Eq. (5).

$$\varepsilon_{ij} = \left(\frac{1+v}{E} + \Phi\right)\sigma_{ij} - \left(\frac{v}{E} + \frac{1}{3}\Phi\right)\sigma_{kk}\delta_{ij} \quad (5)$$

Comparing total strain from Eq. (5) with elastic strain from Eq. (1) total strain can be rewrite as Eq. (6).

$$\varepsilon_{ij} = \frac{1+v_{eff}(x)}{E_{eff}(x)}\sigma_{ij} - \frac{v_{eff}(x)}{E_{eff}(x)}\sigma_{kk}\delta_{ij} \quad (6)$$

In which Φ(*x*) is scalar function that can be achieved from stress-strain curve. $E_{eff}(x)$ and $v_{eff}(x)$ are effective elastic modulus and effective Poisson ratio respectively. Comparing Eq. (6) with Eq. (5) the effective elastic modulus and Poisson ratio can be derive as Eq. (7).

$$E_{eff}(x) = \frac{3E(x)}{3+2E(x)\Phi} \qquad v_{eff}(x) = \frac{3v(x)+E(x)\Phi}{3+2E(x)\Phi} \quad (7)$$

By eliminating Φ(x) from Eq. (7) the Poisson ratio is obtained by Eq. (8)

$$v_{eff}(x) = \frac{E_{eff}(x)(2v(x)-1)+E(x)}{2E(x)} \quad (8)$$

For calculation of effective Poisson ratio and effective elastic modulus the initial elastic solution should be considered. After finding effective elastic modulus and Poisson ratio, the vessel could divided to several thin strips and each strip can be assumed homogenous. Assembling all elements due to their boundary condition of continuity in pressure and displacement of strips as shown in Fig. 2 is resulted finding stress distribution.

For finding effective elastic modulus energy method and projection method can be used. In this research projection method employed finding effective elastic modulus.

2.2. *Projection Method*

In this method the solution of a boundary value problem used as a base to generate inelastic solution. Assuming that each inelastic solution is lower than elastic solution and using the initial elastic solution, the stress-strain cure continued in elastic solution till achieving equivalent strain in point (a) as shown in Fig 3. Then the elastic curve in plastic region decrease with constant strain till arriving point (a') and cut the actual material behavior in plastic region. From *origin to (a') another repetition occurred and this repetition continued until full converge happened.*

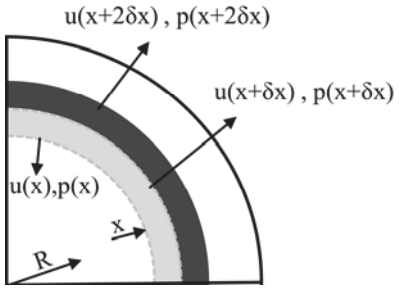

Fig. 2. Schematic of vessel shows continuity in boundary condition of displacement and pressure adjunct thin element as vessel subject to internal pressure

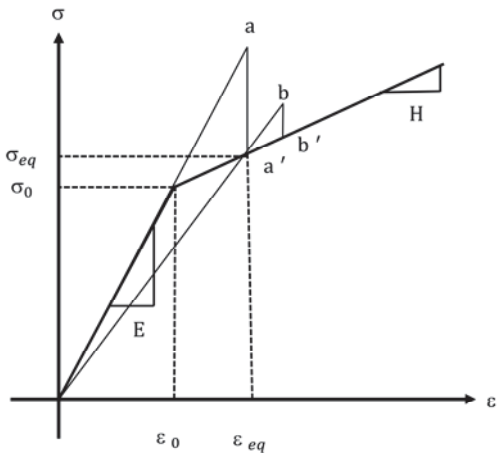

Fig. 3. Stress-strain curve describe projection method for bilinear material

Bilinear behavior is assumed for FGM in elastic-plastic region, as shown in Fig 3. Using this illustration, the equivalent stress is given by

$$\sigma_{eq} = H\left(\varepsilon_{eq} - \varepsilon_0\right) + \sigma_0 \quad (9)$$

In which H, σ_0 and ε_0 are tangent modulus, yield stress and yield strain respectively. The effective elastic modulus can be obtained as Eq. (10).

$$E_{eff} = \frac{\sigma_{eq}}{\varepsilon_{eq}} \quad (10)$$

σ_{eq} and ε_{eq} are equivalent stress and equivalent strain, respectively. Using Eq. (9) and Eq. (10) the effective elastic modulus can be obtained as Eq. (11).

$$E_{eff}(x) = \frac{H(\varepsilon_{eq} - \varepsilon_0) + \sigma_0}{\varepsilon_{eq}} \quad (11)$$

The effective Poisson ratio for each element, $v_{eff}(x)$, is obtained using Eq. (8). In the next step, the state of stress in each element is recalculated using the updated values of effective elastic modulus and effective Poisson ratio. This procedure is continued until the convergence is achieved. This numerical procedure gives a close estimate of the elasto-plastic stresses in the structure.

2.3. *VMP Method for Spherical Vessel*

Fig. 4 shows a spherical vessel of inner radius R, and thickness t, with a spherical strip element designated at a distance x from inner radius of vessel with thickness of dx. In order to evaluate the state of stress in the thick FGM spherical vessel, the displacement distribution is taken as given by Eq.(12) [9].

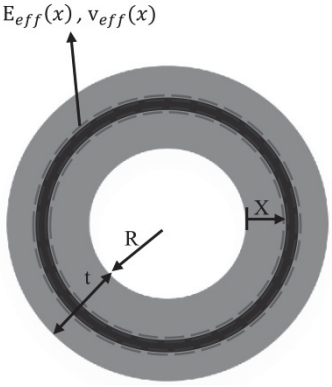

Fig. 4. Schematic of vessel with varying material property[10]

$$\begin{bmatrix} c_{11,x} & c_{12,x} \\ c_{21,x} & c_{22,x} \end{bmatrix}^{-1} \begin{pmatrix} u_x \\ u_{x+dx} \end{pmatrix} = \begin{pmatrix} p_x \\ p_{x+dx} \end{pmatrix} \quad (12)$$

in which p_x and p_{x+dx} are internal and external pressure and u_x and u_{x+dx} are internal and external radial displacement of each strip. C_{ij} matrix can be found from Lamé's equations [9, 11] as given in Eq. (13)

$$c_{11,x} = \frac{(R+x)^4(1-2v_{eff}) + (R+x+dx)^3(R+x)}{E_{eff}((R+x+dx)^3 - (R+x)^3)}$$

$$c_{12,x} = \frac{(R+x)(R+x+dx)^3(2-2v_{eff})}{E_{eff}((R+x+dx)^3 - (R+x)^3)}$$

$$c_{21,x} = \frac{(R+x+dx)(R+x)^3(2-2v_{eff})}{E_{eff}((R+x+dx)^3 - (R+x)^3)} \quad (13)$$

$$c_{22,x} = \frac{(R+x+dx)^4(2v_{eff}-1) + (R+x)^3(R+x+d}{E_{eff}((R+x+dx)^3 - (R+x)^3)}$$

Assembling all elements together Eq. (14) drives.

$$[C'][U] = [P] \quad (14)$$

The stress distribution in each thin strip can be obtained from thick elastic solution of spherical vessel using Eq. (15).

$$\sigma_r = \frac{P_x(R+x)^3 - P_{x+dx}(R+x+dx)^3}{(R+x+dx)^3 - (R+x)^3} - \frac{(R+x)^3(R+x+dx)^3(P_x - P_{x+dx})}{R^3((R+x+dx)^3 - (R+x)^3)}$$

$$\sigma_\theta = \sigma_\Phi = \frac{P_x(R+x)^3 - P_{x+dx}(R+x+dx)^3}{(R+x+dx)^3 - (R+x)^3} - \frac{(R+x)^3(R+x+dx)^3(P_x - P_{x+dx})}{R^3((R+x+dx)^3 - (R+x)^3)} \quad (15)$$

In which σ_r and σ_θ are radial and hoop stress. Stress distribution for thick vessel can be obtained by soperposing stress of all elements.

3. Residual Stress

Residual stress can be obtained by superposing stress distribution for loading and unloading phase using Eq. (16).

$$\sigma_{ij}^R = \sigma_{ij}^l - \sigma_{ij}^u \quad (16)$$

σ_{ij}^R, σ_{ij}^l and σ_{ij}^u are residual stress, loading stress and unloading stress.

The unloading solution is analogous to loading except that each element has a specific nonlinear unloading behavior which depends on the element's equivalent stress at the onset of unloading and also the material hardening behavior. In isotropic hardening behavior, which is shown in Fig. 5, the yield strength of unloading phases can be obtained by Eq. (17).

$$\sigma_0^u = 2\sigma_{max} \quad (17)$$

σ_0^u and σ_{max} are unloading yield strength and maximum stress in loading phase respectively. In reloading phase after autofrettage process the induced residual stress cause a break in equivalent stress which postponed vessel failure.

4. FGM Structure

Based on the rule of mixtures, Tamura *et al.* [12] proposed a simple and applied (TTO) model to describe the stress-strain curves of functionally graded materials. The TTO model couples the uniaxial stress (σ) and strain (ε) of the composite to the corresponding average uniaxial stresses and strains of the ceramic and metal that shows by Eq. (18)

$$\sigma = f_c\sigma_c + f_m\sigma_m \qquad (18)$$
$$\varepsilon = \mathrm{f_c}\varepsilon_c + f_m\varepsilon_m$$

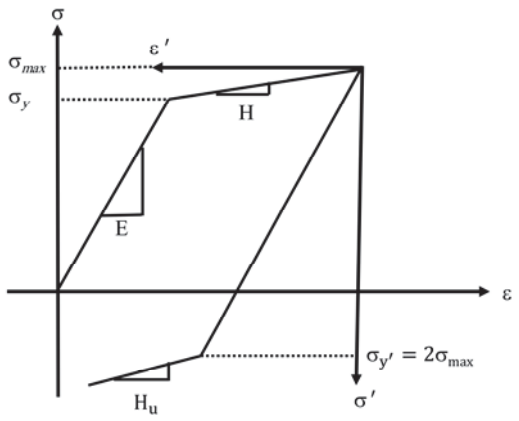

Fig. 5. Bilinear material under unloading for isotropic hardening[5]

Where f_c and f_m are volume fraction of ceramic and metal respectively. The volume farction relation of ceramic and metal can be describe by Eq. (19)

$$f_c + f_m = 1 \qquad (19)$$

The TTO model introduces new parameter, q, to represent the ratio of stress to strain transfer shows by Eq. (20)

$$q = \frac{\sigma_c - \sigma_m}{\varepsilon_c - \varepsilon_m} \qquad 0 \le q \le \infty \qquad (20)$$

Young's modulus of FGM can be obtained from Eq. (21)

$$E_{com} = \left[f_m E_m \frac{q + E_c}{q + E_m} + (1 - f_m)E_c\right] \times \left[f_m \frac{q + E_c}{q + E_m} + (1 - f_m)\right]^{-1} \qquad (21)$$

in which E_{com}, E_m and E_c are elastic modulus of FGM and metal and ceramic respectively. For TTO model ceramic is assumed to have fully linear elastic behavior, and metal and FGM assumed to have bilinear behavior in elastic-plastic region as seen in Fig. 6. The yield stress of the FGM is given by Eq. (22)

$$\sigma_y = \sigma_{ym}\left[f_m + \frac{q + E_m}{q + E_c}\frac{E_c}{E_m}(1 - f_m)\right] \qquad (22)$$

σ_y and σ_{ym} are yield strength of FGM and metal respectively. Tangent modulus For FGM in plastic region obtained by assuming linear behavior for metal in plastic region by Eq. (23)

$$H_{com} = \left[f_m H_m \frac{q + E_c}{q + H_m} + (1 - f_m)E_c\right] \times \left[f_m \frac{q + E_c}{q + H_m} + (1 - f_m)\right]^{-1} \qquad (23)$$

The ultimate strength of FGM can be obtained by Eq. (24)

$$su_{com} = f_c su_c + f_m su_m \qquad (24)$$

In which su_{com}, su_m and su_c are ultimate strength of FGM, metal and ultimate tensile strenght of ceramic respictively[13].

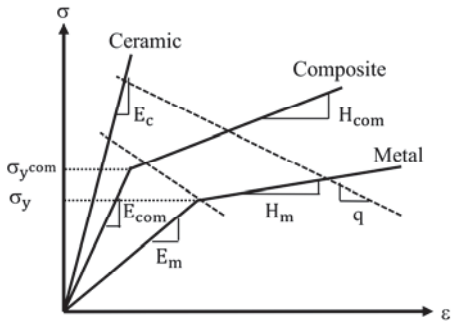

Fig. 6. Rule of mixtures used to estimate the behavior of ceramic-reinforced metal composite based on the ceramic volume fraction in composite for TTO model[12]

The materials property that use in this research shown in table 1.

5. Results

For parametric analyzing, inner and outer radius of FG vessel assumed to be constant (r_i=50 Cm and r_o=100 Cm). First the effect of FGM parameters investigated on amount of pressure capacity and then the effect of autofrettage process are discussed. The effect of each parameter is discussed separately by assuming constant value for others.

.

Table 1. Properties of metal and ceramic used in FGM [14, 15]

Material properties	Alumina	Aluminum
Young's modulus (GPa)	375	71
Poisson's ratio	0.33	0.33
Yield Strength (MPa)	------	503
Ultimate strength (MPa)	379	573
Tangent modulus (GPa)	-------	11
Density (gr/cm^3)	3.89	2.8

5.1. *Validation*

In order to examine the validity of the VMP, a homogenous A237 steel vessel is considered. Properties of steel are taken to be: Young modulus=209 GPa, Poisson's ratio=0.33, yield strength=1100 MPa, ultimate tensile strength=1250 MPa, tangent modulus=10 GPa, density=7.3 gr/cm^3. Using an autofrettage pressure of 1300 MPa, the distribution of residual hoop stress using VMP is shown in Fig. 7 and is compared with that of Ref. [6]. As it is seen, there is a good match between these results. The distributions of residual radial and equivalent stresses obtained from VMP are also shown in the figure. As it is seen, the residual radial stress is not much affected by autofrettage process, and is almost close to zero everywhere.

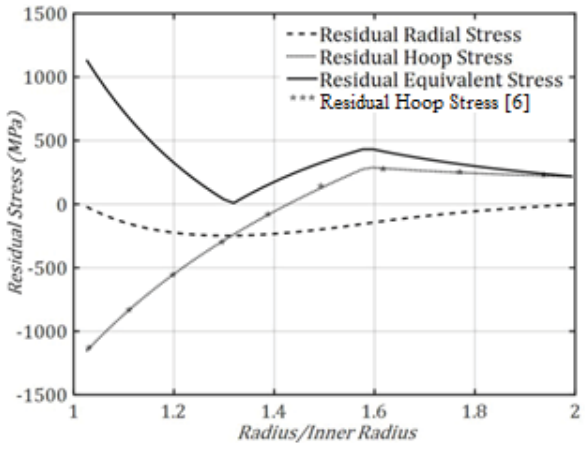

Fig. 7 Residual radial, hoop and equivalent stress distribution after autofrettage of the thick homogeneous spherical vessel with r_o/r_i=2

5.2. *Effect of FGM Parameters*

Aluminum and alumina are used for metal and ceramic in FGM, which is mentioned in table 1. Volume fraction of ceramic that used in outer layer of vessel (f_0) is one of the most significant parameter which related directly to amount of beneficial induced residual stress at inner surface of vessel. Ultimate strength of ceramics are mostly lower than metals which cause negative effect of using high volume fraction of ceramic on pressure capacity of vessel. The second important parameter which is explaining distribution of ceramic particle in thickness of vessel is (n). Relation between (f_0) and (n) and their range of variation is given by [16] :

$$f(x) = f_0\left(\frac{x}{t}\right)^n \qquad 0 \le f_0 \le 1 \ ، \ 0 \le n \le 3 \tag{25}$$

where, x and t are Radial coordinate and thickness of vessel respectively. The third parameter that was introduced by TTO model is stress to strain transfer ratio (q) that mentioned in Eq. (20). The initial value for this parameter as suggested by TTO model is assumed (q=17200).

5.2.1. *Effect of f_0*

In the case of linear distribution for ceramic particle (n=1) and in the absence of autofrettage pressure, the effect of ceramic volume fraction is investigated. The value of q is taken to be 17200. Fig. 8 shows the effect of ceramic volume fraction on pressure capacity of vessel. (f_0=0) illustrates homogenous metal vessel which has 470 MPa pressure capacity and (f_0=1) illustrates using full ceramic volume fraction in outer radius of vessel with linear distribution of ceramic which has a pressure capacity of 580 MPa. Parametric analyzing offer better configuration (f_0=0.9 and n=1) in which pressure capacity is increased up to 610 MPa. In Fig. 8, the break and drop in pressure capacity after (f_0=0.9) proves that using high volume fraction of ceramic because of its low ultimate strength is not beneficial.

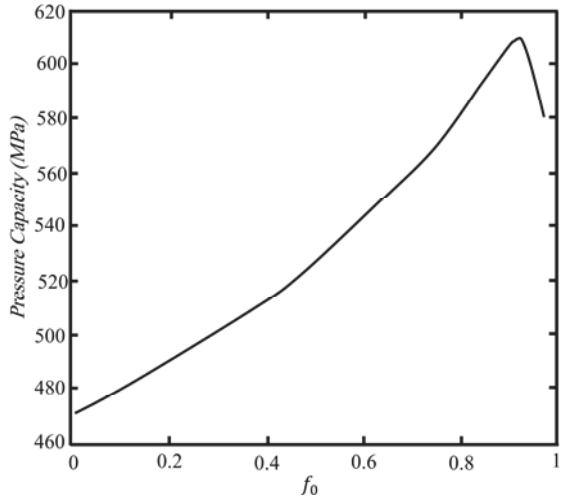

Fig. 8. Effect of volume fraction of ceramic particle (f_0) on outer surface of spherical FGM vessel on pressure capacity

5.2.2. *Effect of n*

With assumption of using full ceramic volume fraction (f_0=1) and absence of autofrettage pressure and assuming q=17200, the effect of power index distribution of ceramic particle is investigated. Fig. 9 shows the effect of *n* on pressure capacity of vessel. n=0 corresponds to homogenous ceramic vessel which has only 250 MPa pressure capacity. The best value for *n* in this configuration is n=0.93, which increases pressure capacity up to 596 MPa. As it was seen, *n* and f_0 are related to each other by Eq. (25). Therefore, analyzing the combined effects of *n* and f_0 is necessary.

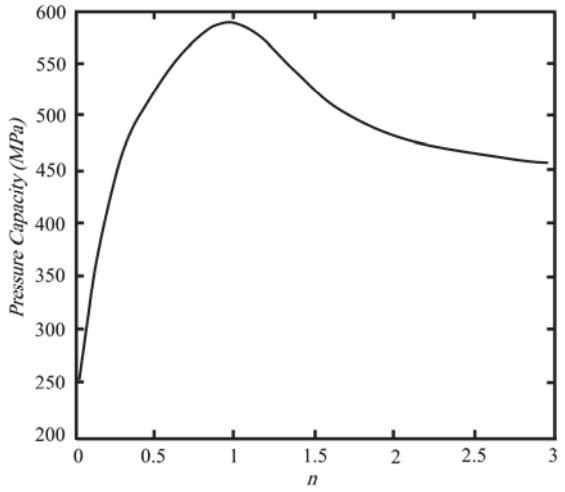

Fig. 9. Effect of power index of ceramic particle (n) of spherical FG vessel on pressure capacity

5.2.3. *Combined effect of n and f_0*

Fig. 10 shows the effect of both *n* and f_0 on pressure capacity of vessel create three-dimensional graph in which f_0=0 illustrates homogenous metal vessel.

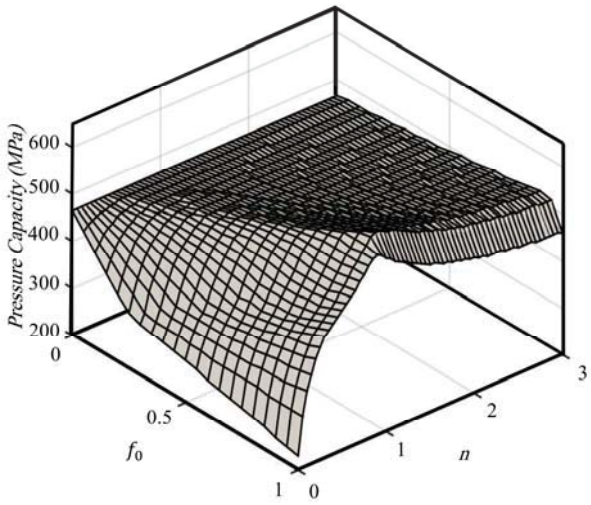

Fig. 10. Combined effect of power index of ceramic particle (n) and volume fraction of ceramic particle (f_0) on pressure capacity of spherical FG vessel

From this figure, a configuration of n=1.05 and f_0=0.95 offers an increased pressure capacity up to 618 MPa. The results illustrate that using beneficial mount of ceramic particle can increase pressure capacity up to %31.

5.2.4. *Effect of q*

For analyzing the effect of parameter *q* on pressure capacity of the vessel, the results of pervious investigation (n=1.05 and f_0=0.95) are used. The results of analyzing this parameter is shown in Fig. 11. The best value for this parameter can be chosen in the range of 35000≤q≤40000. The high value for this parameter according to TTO model, suggests constant stress in FGM. Using suggested values for (*q*) increases the pressure capacity up to 623 MPa.

5.3. *Effect of Autofrettage Pressure (P)*

The fourth parameter that has significant effect on residual stress and pressure capacity is autofrettage pressure which sets the plastic region. As it is seen in Fig. 12, autofrettage pressure can increase from zero up to a pressure that causes vessel failure.

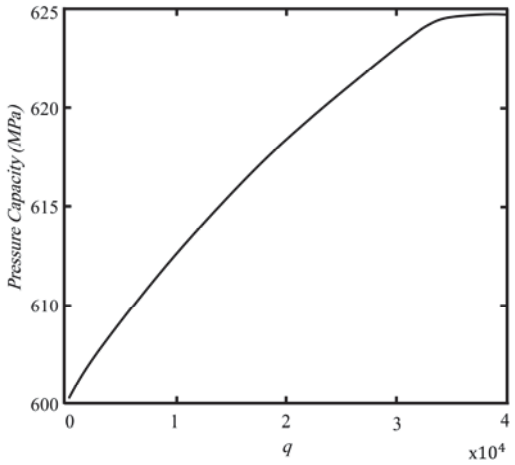

Fig. 11. Effect of parameter q on pressure capacity of FGM spherical vessel

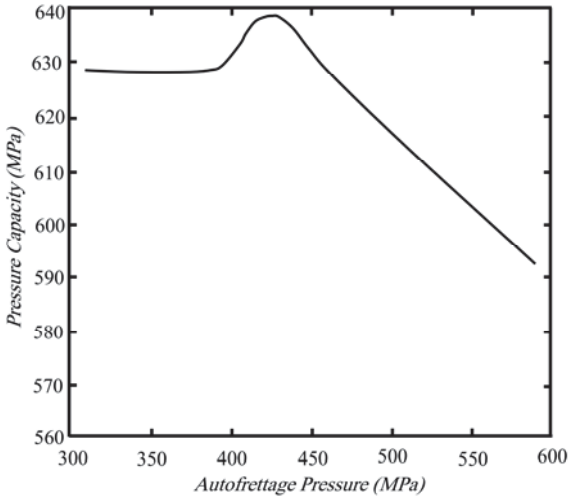

Fig. 12. Effect of autofrettage pressure on load capacity of spherical FG vessel

By increasing the autofrettage pressure up to 400 MPa, there is hardly a plastic deformation developed in inner radius of vessel and pressure capacity does not change. By increasing the autofrettage pressure to 440 MPa, beneficial residual stress is induced in vessel that causes pressure capacity to increase up to 637 MPa. After this autofrettage pressure, the vessel starts failing and pressure capacity drops.

6. Conclusions

The pressure vessels could be divided as thin and thick vessel. For achieving higher pressure thick vessel could be used. For thick vessels, stress distribution of loading is very little at outer surface of vessel but the vessel going to fail from inner surface, in this case using residual stress can be beneficial for Postponed failing by creating better stress distribution. The magnitude of ceramic volume fraction use in vessel, effects on mount of residual stress and pressure capacity. Although using ceramic particle cause achieving higher residual stress and higher pressure capacity but lower ultimate strength of ceramic cause drops in pressure capacity. This parametric analyzing help to find beneficial mount of ceramic that should be used in FGM. The suggested configuration with ($n=1.05$, $f_0=0.95$, $35000 \leq q \leq 40000$ and $P=440$ MPa) increase pressure capacity of vessel up to 35% compared to full metal case and 154% compared to full ceramic case and 10% compare to linear distribution of ceramic particle for FGM. Compare to pervious research which assumed linear distribution for ceramic particle in FGM, in this paper with parametric analyzing of FGM behavior and autofrettage pressure 10% growth in pressure capacity achieved.

7. References

[1] Thumser. R,Bergmann.JW, Vormwald.M., 2002, Residual stress fields and fatigue analysis of autofrettaged parts, Int J of Pressure Vessels and Piping 79(4): 113-117.

[2] Parker.AP, Hara.GP, Underwood.JH., 2003, Hydrulic versus swage Autofrettage and implications of the Bauschinger effect, Pressure Vessel Technol, 5(125): 309-314.

[3] Farrahi.GH, Voyiadjis.GZ, Hoseini.SH, Hosseinian.E., 2013, Residual Stress Analysis of the Autofrettaged Thick-Walled Tube Using Nonlinear Kinematic Hardening, J of Pressure Vessel Technology 135(4): 41-48.

[4] Farrahi.GH, Voyiadjis.GZ, Hoseini.SH, Hosseinian.E., 2012, Residual stress analyses of re-autofrettaged thick-walled tubes., *International Journal of Pressure Vessels and Piping* 98(5): 57-64.

[5] Adibi-Asl.R, Livieri.P., 2007, Analytical Approach in Autofrettaged Spherical Pressure Vessels Considering the Bauschinger Effect, J of Pressure Vessel Technology 129(4): 411-419.

[6] Maleki.M, Farrahi.GH, Haghpanah.Jahromi.B, Hosseinian.E., 2010, Residual stress analysis of autofrettaged thick-walled spherical pressure vessel, Int J of Pressure Vessels and Piping 87(4):396-401.

[7] Haghpanah.Jahromi.B, Farrahi.GH, Maleki.M, Nayeb-Hashemi.M, Vaziri.A., 2009, Residual stresses in autofrettaged vessel made of functionally graded material, J of Engineering Structures 31(4):30-35.

[8] Jahed.H, Sethuraman.R, Dubey.RN., 1997, A variable material property approach for solving elastic-plastic

problems, Int J of Pressure Vessels and Piping 71(5):285-291.

[9] Timoshenko.SP, Goodier.JN., 1967, The Mathematical Theory of Elasticity, McGraw-Hill, Oxford University Press, Second Edition.

[10] Haghpanah.Jahromi.B, Ajdari.A, Nayeb-Hashemi.H, Vaziri.A., 2010, Autofrettage of layered and functionally graded metal ceramic composite vessels, J of Composite Structures 92(7): 813-822.

[11] Sadd.MH., 2009, Elasticity Theory, Applications, and Numerics ,Elsevier Scince, third Edition ,

[12] Tamura.I, Tomota.Y, Ozawa.H., 1973, in: Strength and ductility of Fe-Ni-C alloys composed of austenite and martensite with various strength, in 3rd International Conference on Strength of Metals and Alloys, Institute of Metals,Cambridge: 611-615.

[13] Miyamoto.Y, Kaysser.WA, Rabin.BH, Kawasaki.A., 1999, Functionally Graded Materials: Design, Processing, and Applications, Kluwer Academic Landan,Second Edition.

[14] *Aluminum Alloy*, Accessed on july 2014 ; http://asm.matweb.com/search/SpecificMaterial.asp.

[15] *Properties For Alumina* Accessed on September 2013 ; http:// www.accuratus.com.

[16] Suresh.S, Mortensen.A., 1998, Fundamentals of functionally graded materials: processing and thermomechanical behaviour of graded metals and metal-ceramic composites, IOM Communications Ltd, London,Third Edition.